Shape analysis of Iron Age sheep astragali suggests west-to-east morphotype diffusion in the southern Levant

Sierra A. Harding[1] and Nimrod Marom[1*]

[1] Laboratory of Archaeozoology, School of Archaeology and Maritime Cultures, University of Haifa.

Abstract

We examine the possibility that expanding trans-Mediterranean trade during the Iron Age (ca. 1,000–350 BCE) has resulted in increased morphological variability among sheep from maritime sites in the southern Levant. Using geometric morphometric tools, we compared the variability in sheep astragal morphology in a port settlement on the Carmel coast (Tel Dor), a coastal settlement in the Akko valley (Tell Keisan), and an inland urban settlement in the Hula Valley (Tel Abel Beit Maacah). Our results suggest that the sheep astragali from the port settlement at Tel Dor occupy a significantly different part of shape space than the specimens examined from the two other sites. In addition, a source-sink dynamic is implied by the appearance of coastal morphotypes in the inland site, whereas unique inland morphotypes do not occur at the coastal site. This findings do not contradict the possibility of maritime importation and consequent overland spread of non-local sheep variants in the southern Levant during the heyday of 'Phoenician' trade.

Introduction

Livestock mobility is a multifaceted phenomenon relating to expansion, demographic growth, and genetic/phenotypic variability. Traditionally, most studies on livestock mobility focused on the spread of newly domesticated animals across space and through time (Daly et al., 2018; Davis & Simões, 2016; Krause-Kyora et al., 2013; Ottoni et al., 2013). In recent years, however, attention has also turned to later period movement of livestock using techniques like ancient DNA and geometric morphometrics, which allow us to perceive some of the "Brownian motion" that has fashioned much of the genetic and phenotypic patterns in ancient livestock (Colominas Barberà et al., 2019; Evin et al., 2015; Haruda et al., 2019). By tracing subtle dissimilarities between animals from different times and locales, such techniques allow to track variability among and between ancient animal populations. In this paper, we use geometric morphometrics to address the subject of maritime connectivity and livestock mobility, postulating that access to maritime networks creates coastal sources of phenotypic diversity that can percolate to sinks in inland regions (Muñiz et al., 1995; Valenzuela-Lamas et al., 2018). In other words, we assume that maritime livestock mobility could produce a distinctive morphological signature in seaside settlements, and perhaps a diffusive cline of such morphotypes to settlements remote from the coast. To explore this idea, we intend to use a standard protocol applied to sheep astragali (Pöllath et al., 2019), assuming that these small ungulates would have been traded as breeding stock for their secondary products, especially wool.

Our case study is located in the Iron Age 2 and the Persian period (9th-5th centuries BCE) southern Levant, in what is today northern Israel. This region has been partially under the sway of the Kingdom of Israel and of the coastal city of Tyre in a time period when cross-Mediterranean maritime connections stretched out from the Levantine coast to the Pillars of Melkert (Brody, 2002; Broodbank, 2013; Eshel et al., 2018). We expect that the hub of this extensive maritime network would have received exotic trade goods from a distance, including sheep livestock, and therefore provide a suitable setting to explore the link between maritime connectivity and livestock mobility. We focus our efforts on three assemblages from this region and period: Iron Age 2 (9th to 6th centuries BCE) Tel Dor, an important port south of Mt.

Carmel (Gilboa & Sharon, 2003); Tel Abel Beth Maacah (9th to 6th centuries BCE), an inland town in the Hula Valley, north of the Sea of Galilee (Yahalom-Mack et al., 2018); and Iron Age 2 to Persian period Tel Keisan (9th to 4th centuries BCE), which is located between the Galilee coast and foothills (Humbert, 1981; Schipper, n.d.). These sites were chosen because they are in different degrees of remoteness from the sea, and because they have a fair number of astragali from Iron Age contexts, some of which could be identified as sheep. Our assumption is that the morphology of sheep astragali at the port site of Tel Dor will be different from that of the inland site of Tel Abel Beth Maacah, with coastal Tel Keisan assuming an intermediate position. In other words, we expect a west-to-east morphocline. If our assumption is wrong, there will be no such effect, and sheep morphologies will be similar between the different sites, which are less than 100 km apart.

Specialists in the archaeology of the Iron Age Levant are used to a high, almost decadal-scale temporal resolution obtained from radiocarbon dating and very refined ceramic chronologies; to them, the five centuries spanned by our sample may look inapt. We can answer such concerns in two ways. The first is by noting the trivial fact that we must pool chronostratigraphic phases in order to even remotely approach a liminal sample size of complete sheep astragali from each site. The second, which is less trivial, is that we should not assume that the pace of spread of livestock morphotypes is related in any way to the pace of change in ceramic assemblages on which archaeological chronostratigraphy is ultimately based. On the contrary, cultural evolution is rapid in comparison to biological evolution. We therefore think that the scale of time represented by our samples, which spans a few centuries after the post Bronze Age collapse explosion of trans-Mediterranean trade, is essentially correct, to an order of magnitude, for observing the more "viscous" spread of sheep morphotypes.

Be the case as it may, we do not pertain to having surmounted the issue of insufficient sample sizes and unresolved spatiotemporal scales in our study. Our results, which represent the first study of animal mobility in the southern Levant using geometric morphometric methods, should be taken with a grain of salt.

Materials

The GMM analysis was conducted on a sample of sheep astragali that were osteologically mature at time of death, as well as free from surface damage, modifications, burning, pathology, or other anomalies that would inhibit comparison using digital landmarks. Skeletal elements were visually identified as *Ovis* sp. using morphological criteria (Boessneck, 1970; Zeder & Lapham, 2010) and the comparative collection at the Laboratory for Archaeozoology at the University of Haifa.

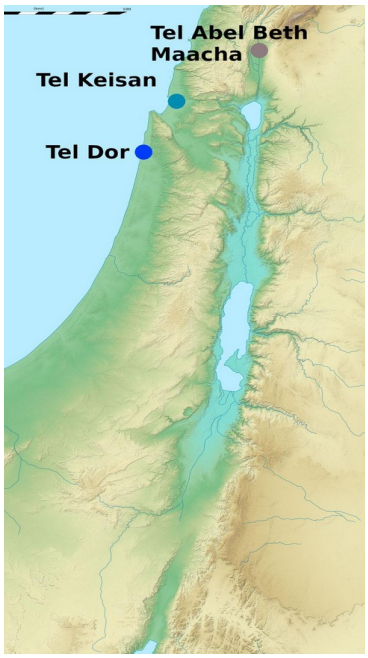

Figure 1: Site location map. Base map by Eric Gaba, Wikimedia Commons.

The sample comprises Iron Age 2 Abel Beth Maacah (ABM, N=87); Iron Age 2 Tel Dor (Dor, N=14); and pooled Iron Age 2 Keisan (Keisan, N=8) and Persian Keisan (Keisan, N=11) ; Figure 1). Although every effort was made to achieve a spatiotemporally balanced dataset for this analysis, the diverse zooarchaeological assemblages included in this study are not homogenous with respect to the sample size from each site and time period. In the case of Dor, we analyzed a sample of N<15. Smaller sample sizes have been shown to be less statistically powerful in previous analyses and the results produced here should be interpreted with caution (Cardini et al., 2015; Pöllath et al., 2019). It is also worth noting that the astragali from ABM were recovered from a jar that held more than 400 astragali of diverse artiodactyls (Susnow et al., 2021), while the specimens from other sites were derived from refuse layers in a settlement context.

Methods

Digitization. Digital photographs of the anterior surface of each astragalus were taken in ambient lighting with a Nikon D7500 using an AF-S Nikkor 40mm lens by lab technician Roee Shafir. The camera was stabilized on the photography table using a 90^{o} stable arm. For each photo, the

4

astragalus was placed in a sand-filled box and a bubble level was used to ensure that the surface was horizontal. A 1 cm scale was placed at the level of the photographed surface. The dataset of digital photos was imported into tpsUtil (v.147) (J. Rohlf, 2015). Digitization of landmarks was conducted by laboratory assistant Daria Loshkin Gorzilov, under the direct supervision of S. Harding, using tpsDig232 (v.231) (J. F. Rohlf, 2017). We preferred left-side elements; images of right-side elements were flipped in tpsDig 232. The landmark configuration followed the protocol outlined in Pöllath et al. (2019): 11 fixed landmarks (LM) and 14 semi-sliding landmarks (SSLM) were placed around the outline of the dorsal view (Fig. 2). A scale was set for each photo within tpsDig.

Digitization error. Digitization errors were checked before statistical analysis by using tpsSmall64 (v.1.0) and tpsrelw32 (v.1.53) (Rohlf, 2015) according to the protocol described by (Adriaens, 2007). A subset (N=28) of specimens from the dataset were digitized three unique times in order to test for digitization error; these were randomly selected but as evenly distributed between the study sites as possible.

Generalized Procrustes analysis. A Generalized Procrustes Analysis (GPA) was performed using the gpagen() function in 'geomorph' (Adams et al., 2022; Adams & Otárola-Castillo, 2013) on the landmark coordinates obtained in tpsDig which produced Procrustes shape variables (Bookstein, 1991). SSLM's were allowed to slide relative to each other during the GPA in order to minimize the sum Procrustes distances between each specimen and the mean shape (Bookstein, 1996). Centroid sizes of the specimens were also produced by the same function.

Principal components and disparity analyses. We used principal component analysis (PCA, implemented using the gm.prcmp() function in 'geomorph') to reduce the dimensionality of the Procrustes transformed landmarks, while retaining most of the variability present among the Procrustes shapes. In addition to an interpretation of first and second principal component biplot, we also applied a descriptive disparity analysis aimed to characterize the differences between the groups based on their size and their positions (Guillerme, Cooper, et al., 2020; Guillerme, Puttick, et al., 2020): Disparity analysis appeals to us for its simplicity and its generalized, geometric approach to morphological trait space. The first ten principal component scores of the specimens were treated as points in a multi-dimensional trait space, where disparity in the size, density, and positions of the different groups could be calculated. The *size* of a group

5

approximates the amount of trait space it occupies; larger volumes indicate the presence of more extreme trait combinations (i.e., higher variability) in the shapes present in a group. Size disparity was measured (Guillerme, 2018) as the median Euclidean distance from the morphospace centroid along each axis. The *density* of a group relates to the distribution of the observations within the group's discrete trait space; a higher median density means that more specimens in a group will tend to be more similar to each other. Density disparity was measured as the median Euclidean pairwise distance between specimens in a group. The *position* of a group captures where it resides in the trait space relative to the space's origin; different positions represent distinct trait combinations for different groups. Position disparity was measured using average displacements, calculated as the ratio between the median Euclidean distance of the group members to the centroid of each group and to the origin of the space. Median values produced in these calculations were bootstrapped with random replacement (N=100).

R libraries. GMM analysis and visualization were conducted in R (v.4.1.0) (R Core Team, 2022) using the following packages: 'dispRity' (Guillerme, 2018), 'geomorph' (Adams et al., 2022; Adams & Otárola-Castillo, 2013), 'tidyverse' (Wickham et al., 2019), and 'ggsci' (Xiao, 2018).

Data availability. Specimen catalogue, landmark configurations, and R code appear in Supplement 1.

Results

Digitization error. Landmark digitization error (DE) was quantified by calculating the ratio of the mean Procrustes distance of the DE subset (mean=0.034) and the whole dataset (mean= 0.118); the percent of digitization error was 29.37%. This percentage represents the variation in the sample due to imprecision of landmark placement, which does not have a fixed value (Yezerinac et al., 1992, p. 471). This percent of DE is within the range expected for highly morphologically conserved skeletal elements based on other GMM studies (Harding, 2021, p. 59; Hulme-Beaman, 2014, pp. 164–167).

Centroid size. Median centroid sizes extracted by the gpagen() function of the 'geomorph'

package prior to Procrustes transformation are plotted in Figure 2. There is a significant difference in the median size between astragali from the three archaeological contexts, with Tel Keisan producing the largest median (Kruskal-Wallis chi-squared = 9.7027, df = 2, p-value = 0.01). This is in line with the results based on a log-size index analysis of different skeletal elements in coastal and inland Iron Age settlements, which suggest a size increase in Persian period Keisan (Harding et al. in prep.) The greater size of the Keisan specimens suggests to Harding et al. either higher representation of adult male animals in the population, and therefore later age-at-death for this sex group, or the improvement of local livestock.

Disparity. Bootstrapped values for median size, density, and position disparity calculations are presented in Figure 2. The spread of the bootstrapped values is narrow in ABM, and broader in Dor and Keisan, reflecting the large differences in sample sizes between the first and latter assemblages; however, significant differences in disparity parameters between the groups are evident. Disparity *size*, which reflects the spread of the data around group centroids and therefore intra-group morphological variability, is similar for inland ABM and coastal Dor, with Keisan representing slightly less variegated morphologies (Kruskal-Wallis chi-squared = 62.627, df = 2, p-value = 2.516e-14). Disparity *density* is highest at Dor and lowest in Keisan, suggesting less uniform occupation of shape space in Tel Dor; this means that the specimens are more dispersed in trait space in that site, and more closely grouped in Keisan, with ABM assuming intermediate values (Kruskal-Wallis chi-squared = 149.62, df = 2, p-value < 2.2e-16). Lastly, disparity *position*, the distance of group centroids from the origin of the trait space, is much higher in Tel Dor than in the other sites (Kruskal-Wallis chi-squared = 225.51, df = 2, p-value < 2.2e-16). This means that the astragali from Tel Dor occupy a different area of shape space than those from Tel Keisan and ABM; they are morphologically distinct from them in the ten-dimensional trait space.

7

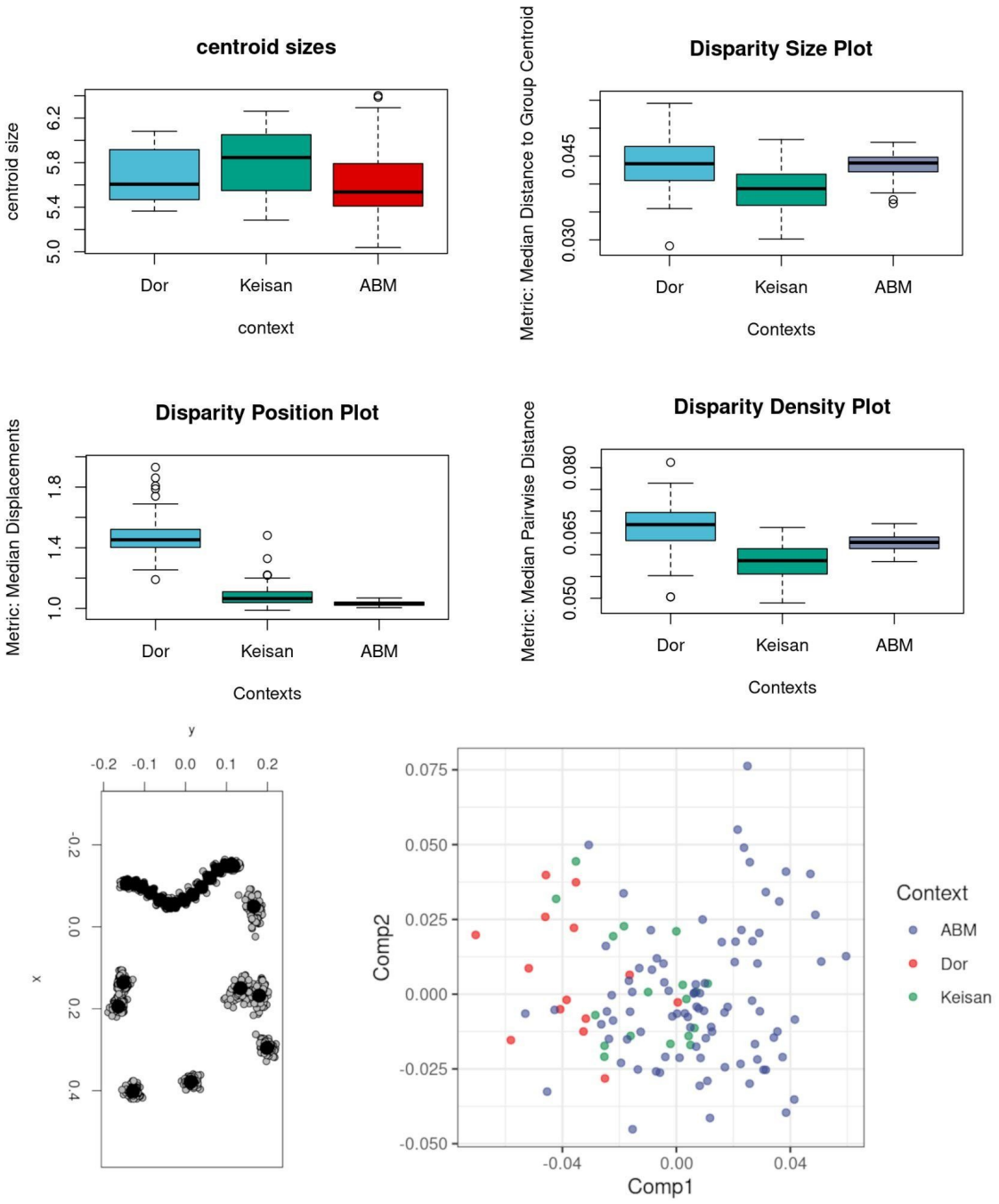

Figure 2: Boxplots present specimen centroid sizes (top left) and bootstrapped (n = 100) median disparity statistics (size, position, and density); A plot of the Procrustes transformed landmarks; a shape PCA biplot (bottom) of astragals from Iron Age 2 Tel Abel Beth Maacha (ABM; n=87), Iron Age 2 Tel Dor (n=14) and Iron Age 2 + Persian period Tel Keisan (n=19).

8

Principle components 1 & 2. We plotted the first two principal components obtained from the shape principle component analysis applied using the gm.prcmp() function in the library 'geomorph' to the Procrustes transformed landmark coordinates. The result, presented at the bottom of Figure 2, shows a remarkable pattern: The specimens from Tel Dor and Tel Keisan occupy the left side of the plot, with the great majority of PC1 scores smaller than zero and none larger than 0.01; Tel Keisan specimens are less spread out than those of Dor. The ABM group, however, behaves differently. Its center of gravity is in the positive range of PC1, but negative values are also very well represented. We understand this pattern to reflect one-way mobility of sheep between the coastal and inland sites: the latter, represented by ABM, receive "coastal morphotypes" (negative PC1 values) while maintaining their own local morphotypes (positive PC1 values). The inland morphotypes, however, are not represented in the coastal assemblages, suggesting a source-sink dynamics of livestock introduction from coastal to inland regions.

Conclusions

Our results suggest distinctive patterns of astragular morphology in the Iron Age 2 and Persian period of contemporary northern Israel. In summary, the seaport of Dor has a large morphological trait space in relation to its sample size, and it is located in a different position than ABM and Keisan. Here, disparity analysis allows us to summarize multiple dimensions that would not be visible in a typical multivariate ordination analysis, and suggests the morphological distinctness of Dor from both other sites, and its internal heterogeneity. Both, we believe, support an interpretation of constant introduction of livestock: The different position by pointing at the divergent overall morphology, and the density by revealing the large range of morphological variation even within Dor itself.

The principal components analysis biplot fleshes out this picture by revealing source-sink dynamics between the coastal and inland sites. Contrary to our original expectations, the inland site is more diverse along the first principal component because it receives morphotypes from the coastal region while retaining native and morphologically distinct forms. These dynamics also explain why, for all the introduced diversity, the *size* disparity metric is similar for Dor and

9

ABM: while the first may have received animals from distant places, the latter held on to an important source of diversity in the form of local morphotypes that did not exist along the coast.

Our interpretation of the results is far from certain, based on fairly small sample sizes and a single geographical transect. It does, however, point at a new direction for further research, and provides solid grounds for further hypothesis testing.

Acknowledgements

We wish to thank Gunnar Lehmann, Ayelet Gilboa, Ilan Sharon and Naama Yahalom Mack for allowing us to work on the materials from Tel Keisan, Tel Dor, and Abel Bet Maacah. We also thank Roee Shafir and Daria Lokshin Gorzilov for their technical assistance with specimen photography and digitization.

Funding

This research was funded by the Israel Science Foundation (252/19).

References

Adams, D. C., Collyer, M. L., Kaliontzopoulou, A., & Baken, E. K. (2022). *Geomorph: Software for geometric morphometric analyses* (version 4.0.4.) [Linux]. https://cran.r-project.org/package=geomorph.

Adams, D. C., & Otárola-Castillo, E. (2013). Geomorph: An R package for the collection and analysis of geometric morphometric shape data. *Methods in Ecology and Evolution / British Ecological Society*, *4*, 393–399.

Adriaens, D. (2007). *Protocol for error testing in landmark based geometric morphometrics*. https://www.scribd.com/document/295867417/Geometric-Morphometrics-protocols-for-Error-Testing

Boessneck, J. (1970). Osteological differences between sheep (Ovis ariea Linné) and goats (Capra hircus Linné). In D. Brothwell & E. Higgs (Eds.), *Science in Archaeology* (pp. 331–358). Praeger.

Bookstein, F. L. (1991). *Morphometric Tools for Landmark Data*. Cambridge University Press.

Bookstein, F. L. (1996). Landmark methods for forms without landmarks: localizing group differences in

outline shape. *Proceedings of the Workshop on Mathematical Methods in Biomedical Image Analysis*, 279–289.

Brody, A. (2002). From the Hills of Adonis through the Pillars of Hercules: Recent Advances in the Archaeology of Canaan and Phoenicia. *Near Eastern Archaeology*, *65*(1), 69–80.

Broodbank, C. (2013). *The Making of the Middle Sea: A History of the Mediterranean from the Beginning to the Emergence of the Classical World*. Thames & Hudson.

Cardini, A., Seetah, K., & Barker, G. (2015). How many specimens do I need? Sampling error in geometric morphometrics: testing the sensitivity of means and variances in simple randomized selection experiments. *Zoomorphology*, *134*(2), 149–163.

Colominas Barberà, L., Evin, A., Campmajó, P., Casas, J., Castanyer i Masoliver, P., Carreras Monfort, C., Guardia, J., Olesti i Vila, O., Pons i Brun, E., Tremoleda i Trilla, J., & Others. (2019). Behind the steps of ancient sheep mobility in Iberia: new insights from a geometric morphometric approach. *Archaeological and Anthropological Sciences, September 2019, Volume 11, Issue 9, Pp 4971--4982*.

Daly, K. G., Maisano Delser, P., Mullin, V. E., Scheu, A., Mattiangeli, V., Teasdale, M. D., Hare, A. J., Burger, J., Verdugo, M. P., Collins, M. J., Kehati, R., Erek, C. M., Bar-Oz, G., Pompanon, F., Cumer, T., Çakırlar, C., Mohaseb, A. F., Decruyenaere, D., Davoudi, H., … Bradley, D. G. (2018). Ancient goat genomes reveal mosaic domestication in the Fertile Crescent. *Science*, *361*(6397), 85–88.

Davis, S., & Simões, T. (2016). The velocity of Ovis in prehistoric times: the sheep bones from Early Neolithic Lameiras, Sintra, Portugal. *O Neolítico Em Portugal Antes Do Horizonte 2020: Perspectivas Em Debate*, *2*, 51–66.

Eshel, T., Yahalom-Mack, N., Shalev, S., Tirosh, O., Erel, Y., & Gilboa, A. (2018). Four Iron Age Silver Hoards from Southern Phoenicia: From Bundles to Hacksilber. *Bulletin of the American Schools of Oriental Research. American Schools of Oriental Research*, *379*, 197–228.

Evin, A., Flink, L. G., Bălăşescu, A., Popovici, D., Andreescu, R., Bailey, D., Mirea, P., Lazăr, C., Boroneanţ, A., Bonsall, C., Vidarsdottir, U. S., Brehard, S., Tresset, A., Cucchi, T., Larson, G., & Dobney, K. (2015). Unravelling the complexity of domestication: a case study using morphometrics and ancient DNA analyses of archaeological pigs from Romania. *Philosophical Transactions of the Royal Society of London. Series B, Biological Sciences*, *370*(1660), 20130616.

Gilboa, A., & Sharon, I. (2003). An Archaeological Contribution to the Early Iron Age Chronological Debate: Alternative Chronologies for Phoenicia and Their Effects on the Levant, Cyprus, and Greece. *Bulletin of the American Schools of Oriental Research. American Schools of Oriental Research*, *332*, 7–80.

Guillerme, T. (2018). dispRity: A modular R package for measuring disparity. *Methods in Ecology and*

Evolution / British Ecological Society, *9*.

Guillerme, T., Cooper, N., Brusatte, S. L., Davis, K. E., Jackson, A. L., Gerber, S., Goswami, A., Healy, K., Hopkins, M. J., Jones, M. E. H., Lloyd, G. T., O'Reilly, J. E., Pate, A., Puttick, M. N., Rayfield, E. J., Saupe, E. E., Sherratt, E., Slater, G. J., Weisbecker, V., … Donoghue, P. C. J. (2020). Disparities in the analysis of morphological disparity. *Biology Letters*, *16*(7), 20200199.

Guillerme, T., Puttick, M. N., Marcy, A. E., & Weisbecker, V. (2020). Shifting spaces: Which disparity or dissimilarity measurement best summarize occupancy in multidimensional spaces? *Ecology and Evolution*, *10*(14), 7261–7275.

Harding, S. A. (2021). *Analysis of the Faunal Remains from the Ma'agan Mikhael B Shipwreck* (N. Marom (ed.)) [MA]. University of Haifa.

Haruda, A. F., Varfolomeev, V., Goriachev, A., Yermolayeva, A., & Outram, A. K. (2019). A new zooarchaeological application for geometric morphometric methods: Distinguishing Ovis aries morphotypes to address connectivity and mobility of prehistoric Central Asian pastoralists. *Journal of Archaeological Science*, *107*, 50–57.

Hulme-Beaman, A. (2014). *Exploring the human-mediated dispersal of commensal small mammals using dental morphology : rattus exulans and rattus rattus* [Paris, Muséum national d'histoire naturelle]. http://www.theses.fr/2014MNHN0031

Humbert, J.-B. (1981). RÉCENTS TRAVAUX A TELL KEISAN (1979-1980). *Revue Biblique (1946-)*, *88*(3), 373–398.

Krause-Kyora, B., Makarewicz, C., Evin, A., Flink, L. G., Dobney, K., Larson, G., Hartz, S., Schreiber, S., von Carnap-Bornheim, C., von Wurmb-Schwark, N., & Nebel, A. (2013). Use of domesticated pigs by Mesolithic hunter-gatherers in northwestern Europe. *Nature Communications*, *4*, 2348.

Muñiz, A. M., Pecharroman, M. A. C., Carrasquilla, F. H., & von Lettow-Vorbeck, C. L. (1995). Of mice and sparrows: Commensal faunas from the Iberian iron age in the duero valley (central spain). *Int. J. Osteoarchaeol.*, *5*(2), 127–138.

Ottoni, C., Flink, L. G., Evin, A., Geörg, C., De Cupere, B., Van Neer, W., Bartosiewicz, L., Linderholm, A., Barnett, R., Peters, J., Decorte, R., Waelkens, M., Vanderheyden, N., Ricaut, F.-X., Cakirlar, C., Cevik, O., Hoelzel, A. R., Mashkour, M., Karimlu, A. F. M., … Larson, G. (2013). Pig domestication and human-mediated dispersal in western Eurasia revealed through ancient DNA and geometric morphometrics. *Molecular Biology and Evolution*, *30*(4), 824–832.

Pöllath, N., Schafberg, R., & Peters, J. (2019). Astragalar morphology: Approaching the cultural trajectories of wild and domestic sheep applying Geometric Morphometrics. *Journal of Archaeological Science: Reports*, *23*, 810–821.

Rohlf, J. (2015). The tps series of software. *Hystrix* , *26*(1), 9–12.

316 Rohlf, J. F. (2017). *TPSdig*.
317 Schipper, B. (n.d.). *Tell Keisan Excavations – Archaeological excavations at the site of Tell Keisan in*
318 *Israel*. Retrieved December 23, 2022, from https://keisan.uchicago.edu/
319 Susnow, M., Marom, N., & Shatil, A. (2021). Contextualizing an Iron Age IIA Hoard of Astragali from
320 Tel Abel Beth Maacah, Israel. *Journal of*. https://journal.equinoxpub.com/JMA/article/view/20597
321 Valenzuela-Lamas, S., Orengo, H. A., Bosch, D., Pellegrini, M., Halstead, P., Nieto-Espinet, A.,
322 Trentacoste, A., Jiménez-Manchón, S., López-Reyes, D., & Jornet-Niella, R. (2018). Shipping
323 amphorae and shipping sheep? Livestock mobility in the north-east Iberian peninsula during the Iron
324 Age based on strontium isotopic analyses of sheep and goat tooth enamel. *PloS One*, *13*(10),
325 e0205283.
326 Wickham, H., Averick, M., Bryan, J., Chang, W., McGowan, L. D., François, R., Grolemund, G., Hayes,
327 A., Henry, L., Hester, J., Kuhn, M., Pedersen, T. L., Miller, E., Bache, S. M., Müller, K., Ooms, J.,
328 Robinson, D., Seidel, D. P., Spinu, V., … Yutani, H. (2019). Welcome to the tidyverse. In *Journal of*
329 *Open Source Software* (Vol. 4, Issue 43, p. 1686).
330 Xiao, N. (2018). *ggsci: Scientific Journal and Sci-Fi Themed Color Palettes for "ggplot2."*
331 https://CRAN.R-project.org/package=ggsci
332 Yahalom-Mack, N., Panitz-Cohen, N., & Mullins, R. (2018). From a Fortified Canaanite City-State to ``a
333 City and a Mother'' in Israel: Five Seasons of Excavation at Tel Abel Beth Maacah. *Near Eastern*
334 *Archaeology*, *81*(2), 145–156.
335 Yezerinac, S. M., Lougheed, S. C., & Handford, P. (1992). Measurement Error and Morphometric
336 Studies: Statistical Power and Observer Experience. *Systematic Biology*, *41*(4), 471–482.
337 Zeder, M. A., & Lapham, H. A. (2010). Assessing the reliability of criteria used to identify postcranial
338 bones in sheep, Ovis, and goats, Capra. *Journal of Archaeological Science*, *37*(11), 2887–2905.

339